Protein Control of the Redox Potential of the Primary Quinone Acceptor in Reaction Centers from *Rhodobacter sphaeroides*†

Eiji Takahashi, Todd A. Wells, and Colin A. Wraight*

Department of Biochemistry and Center for Biophysics & Computational Biology, 419 Roger Adams Laboratory/MC-712, University of Illinois at Urbana−Champaign, 600 South Mathews Avenue, Urbana, Illinois 61801

Received May 9, 2000; Revised Manuscript Received November 9, 2000

ABSTRACT: The role of the protein environment in determining the redox midpoint potential (E_m) of Q_A, the primary quinone of bacterial reaction centers, was investigated by mutation of isoleucine at position 265 of the M subunit in *Rhodobacter sphaeroides*. Isoleucine was changed to threonine, serine, and valine, yielding mutants M265IT, M265IS, and M265IV, respectively. All three mutants, with smaller residues replacing isoleucine, exhibited decreased binding affinities of the Q_A site for various quinone analogues, consistent with an enlargement or loosening of the headgroup binding domain and a decrease in the van der Waals contact for small quinones. In all other respects, M265IV was like the wild type, but the polar mutants, M265IT and M265IS, had unexpectedly dramatic decreases in the redox midpoint potential of Q_A, resulting in faster rates of $P^+Q_A^-$ charge recombination. For both anthraquinone and native ubiquinone, the in situ E_m of Q_A was estimated to be ≈100 and 85 mV lower in M265IT and M265IS, respectively. The effect on $E_m(Q_A)$ indicates destabilization of the semiquinone or stabilization of the quinone. This is suggested to arise from either (i) electrostatic interaction between the partial charges or dipole of the residue hydroxyl group and the charge distribution of quinone and semiquinone states with particular influence near the C4 carbonyl group or (ii) from hydrogen bonding interactions between the hydroxyl oxygen and the $N_\delta H$ of histidine M219, causing a weakening of the hydrogen bond to the C4 carbonyl. The rate of the first electron transfer ($k_{AB}^{(1)}$) in the polar mutants was the same as in the wild type at low pH but decelerated at higher pH with altered pH dependence. The rate of the second electron transfer ($k_{AB}^{(2)}$) was 3−4-fold greater than in the wild type over the whole pH range from 4 to 11, consistent with a larger driving force for electron transfer derived from the lower E_m of Q_A.

The acceptor quinones of bacterial reaction centers (RCs), Q_A and Q_B, perform the function of accumulating two reducing equivalents from one-electron turnovers of the primary photoevents. After two turnovers, these are released from the Q_B site as a single molecule of quinol, and the site is refilled by an oxidized quinone from the membrane pool (*1*, *2*):

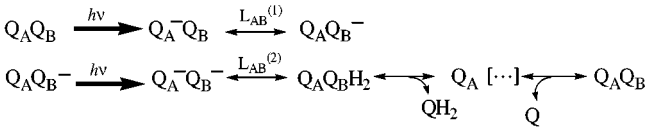

The reductant on both the first and the second electron transfer is Q_A^-, and the electrochemical properties of Q_A and Q_B must be suitably matched to allow this. In many cases, the chemical identity of Q_A and Q_B can be the same, e.g., both are ubiquinone-10 in *Rhodobacter sphaeroides* and both are plastoquinone-9 in Photosystem II of oxygenic photosynthetic organisms. Thus, the distinct physical properties of Q_A and Q_B, including redox potential, are controlled by interactions with the protein environment. In addition to their respective binding pockets in the M and L subunits, there may also be global influences such as long-range interactions that allow—or cause—mutual interactions between the two quinones (*3*).

In the Q_A pocket of RCs from *Rb. sphaeroides*, residue M265 is part of the immediate binding domain of the ubiquinone headgroup, and the wild-type isoleucine is in van der Waals contact with the C3 methoxy group, the C4 carbonyl, and the C5 methyl (see Figure 1) (*4*−*7*). The importance of van der Waals interactions in the binding of Q_A (*8*−*10*) makes it likely that alterations in this residue will affect the binding affinity for quinones. It may also affect physicochemical properties of the in situ quinone through changes in "polarity" of the binding site and possibly through steric influences on the conformation of the methoxy substituents (*11*−*15*). The latter has been proposed to be of importance in tuning the in situ redox potentials of both Q_A and Q_B in *Rb. sphaeroides* reaction centers (*16*). To address some of these questions, we report here the characterization of site-directed mutations of the Q_A site in *Rb. sphaeroides* RCs with isoleucine at position 265 of the M subunit (Ile^{M265}) replaced by the polar residues, threonine and serine, and by an apolar homologue, valine, yielding mutants M265IT, M265IS, and M265IV, respectively. The polar residues were selected rather than more dramatic changes in side chain character, such as ionizable residues, to minimize the

† This work was supported by grants from the National Science Foundation (MCB96-31275 and 99-05672). T.A.W. was supported by a postdoctoral traineeship from the "Integrative Photosynthesis Research Training Program", a NSF GRT program grant (DBI96-02240).

* Corresponding author. Phone: (217)333-3245. Fax: (217)244-6615. E-mail: cwraight@life.uiuc.edu.

10.1021/bi001055g CCC: $20.00
Published on Web 01/03/2001

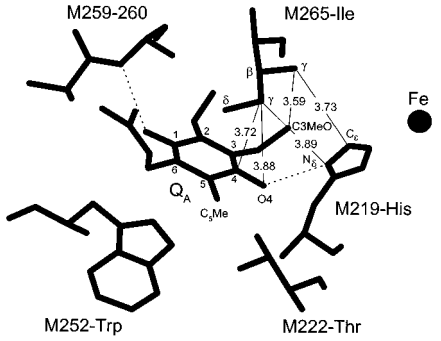

FIGURE 1: Binding pocket of Q_A in the M subunit of reaction centers from *Rhodobacter sphaeroides*. Residues M259 (Asn) and M260 (Ala) are shown as backbone only. The hydrocarbon tail of Q_A is truncated after the first isoprene unit. Hydrogen bonds between the quinone carbonyl oxygens and M260 (peptide NH) and M219 (His-N_δH) are shown as dotted lines. Distances between selected atoms are marked by thin lines and shown in angstroms (values are averages of the structures in refs *6* and *7*).

likelihood of large-scale structural changes. Nevertheless, these mild substitutions had substantial effects on the properties of Q_A, which are discussed in terms of specific influences of the binding site environment.

MATERIALS AND METHODS

The general mutagenesis procedures have been described previously (*17*). The expression strains used are derived from the green, carotenoid-containing strain GA, which is of wild-type constitution apart from terminal steps of the carotenoid synthesis pathway. Site-directed RC mutations were obtained by in vitro mutagenesis (*18*), using oligonucleotides with altered codons for amino acid residue 265 of the M subunit gene. Growth conditions for wild-type and mutant *Rb. sphaeroides* cells as well as the RC preparation procedure have been described previously (*19*). The mutants with threonine and serine substituted at Ile-M265 grew poorly under photosynthetic conditions but were still photosynthetically competent (PS^+).

Quinones were extracted from the RCs by the method of Okamura et al. (*20*) as modified by Gunner et al. (*21*). Binding affinities at the Q_A site, for selected quinones with various ring configurations and substitutions, were determined in isolated RCs, suspended in 0.1% LDAO and 10 mM Tris (pH 8.0) as described (*9*, *21*−*23*). Comparative analyses were based on the methyl and methoxy-substituted naphthoquinones for binding and anthraquinones for kinetics. Quinones were used as provided: ubiquinone (Q-10) and 2-methyl-1,4-naphthoquinone (menadione) were from Sigma, anthraquinone was from Fluka, 1-chloroanthraquinone was from Aldrich, and 1,4-naphthoquinone was from Eastman. 5- and 6-methyl- and 2- and 5-methoxy-1,4-naphthoquinone were generous gifts from K. Warncke, M. R. Gunner, and P. L. Dutton.

Reaction center function was characterized by optical spectroscopy performed on a kinetic spectrophotometer of local design. Measurements of the $P^+Q_A^-$ recombination rates in Q_A-substituted RCs were done in the same buffer used for the quinone reconstitution, 0.1% LDAO and 10 mM Tris (pH 8.0). All other assays were performed in 2.5 mM KCl, 0.02% Triton X-100, 20−40 μM ubiquinone (Q-10), 1 mM buffer(s) (succinate, citrate, Mes, Mops, Tricine, Ches, or Caps, depending on the pH), and 1−2 μM RC.

The kinetics of P^+ dark decay following a flash (charge recombination) were measured at 430 nm. Multiple processes contribute to this net reaction (*21*, *24*−*27*). The term k_P^A is used for the observed rate of recovery of P in the absence of Q_B function ($P^+Q_A^-$ decay), and k_P^B is used for the observed rate of recovery of P in the presence of Q_B ($P^+Q_B^-$ decay).

The kinetics of the first electron transfer from Q_A^- to Q_B were measured at 397 nm. The kinetics of the second electron transfer were monitored at 450 nm with 1−200 μM ferrocene as donor to P^+; 0.5−1 mM potassium ferrocyanide was present to rereduce the ferricenium produced after each flash.

RESULTS

Binding Affinities for Quinone Analogues in the Q_A Site. The parent strain for the M265 mutants is the green, carotenoid-containing GA strain rather than the blue-green carotenoidless R26 strain. These are identical with respect to reaction center proteins, but R26 RCs lack a bound carotenoid. We also compared these two "wild-type" RCs. Binding and function data are shown in Table 1 for selected benzo-, naphtho-, and anthraquinones in the Q_A sites of GA, R26, and the three M265 mutant RCs.

Binding affinities for substituted naphthoquinones have been used to reveal the steric outline of the Q_A binding site

Table 1: Binding and Function of Various Quinone Analogues in the Q_A Site of Two Wild-Type Strains (R26 and GA) of *Rb. Sphaeroides* and Three Q_A Site Mutants: Ile^{M265} → Thr, Ile^{M265} → Ser and Ile^{M265} → Val

	R26			GA			M265IT			M265IS			M265IV		
quinone	K_D (μM)	$\Delta G°$ (kcal/mol)	k_P^A (s^{-1})	K_D (μM)	$\Delta G°$ (kcal/mol)	k_P^A (s^{-1})	K_D (μM)	$\Delta G°$ (kcal/mol)	k_P^A (s^{-1})	K_D (μM)	$\Delta G°$ (kcal/mol)	k_P^A (s^{-1})	K_D (μM)	$\Delta G°$ (kcal/mol)	k_P^A (s^{-1})
ubiquinone-10	$<10^{-3}$	<-12	9.9	nd	nd	9.5	nd	nd	25	nd	nd	22	nd	nd	13.6
ubiquinone-0	9.33	−6.84[a]	2.0												
6-methyl-UQ-0	0.63	−8.43[a]	2.2												
duroquinone	0.26	−8.97	2.0	0.55	−8.51	2.9	2.28	−7.67	8.7	10.6	−6.25	6.3			
naphthoquinone	5.85	−7.12	9.7	3.09	−7.50	9.1	15.4	−6.54	15.0	48.2	−5.84	14.5	9.0	−6.86	9.7
2-methyl-NQ	0.46	−8.62[a]	nd	0.42	−8.68	8.2	2.04	−7.74	7.7	11.3	−6.72	9.2	0.76	−8.32	7.6
5-methyl-NQ	4.43	−7.28[a]	nd	6.29	−7.07	15.1	11.8	−6.70	21.1	49.1	−5.85	18.7			
6-methyl-NQ	0.41	−8.69[a]	nd				1.38	−7.97	15.7	5.97	−7.10	15.2			
2-methoxy-NQ	0.46	−8.62[a]	nd	0.25	−8.98	10.9				4.93	−7.21	30.8			
5-methoxy-NQ	0.61	−8.42[a]	nd	1.29	−8.01	25.6	10.7	−6.76	24.7						
anthraquinone	0.14	−9.31	112	0.12	−9.41	129	0.42	−8.70	6810	1.51	−7.92	3155	0.17	−9.21	102
1-chloro-AQ	0.063	−9.79	27.4	0.07	−9.73	28.4	0.27	−8.93	1950	1.61	−7.88	767	nd	nd	39.8

[a] Data from ref 22. nd, not determined.

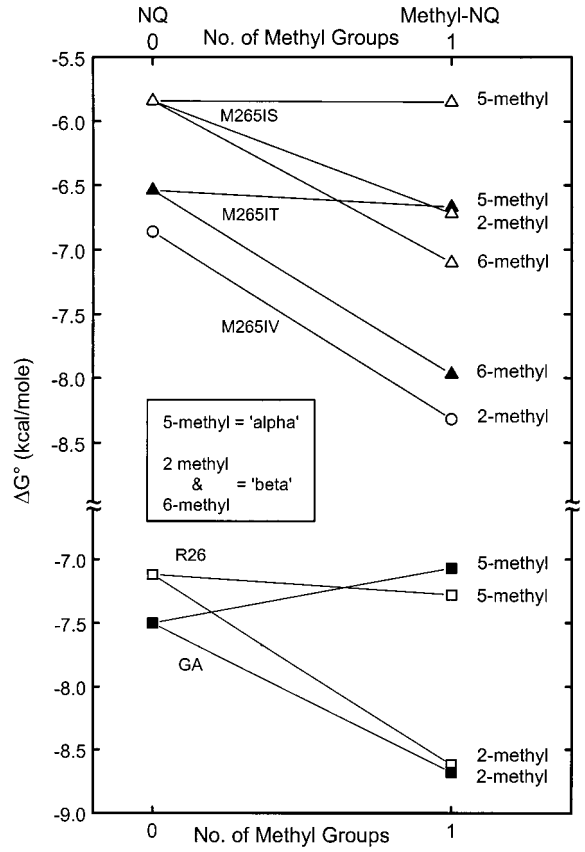

FIGURE 2: Binding affinities for 1,4-naphthoquinone and methyl-naphthoquinones in wild-type and mutant reaction centers: (△) M265IS, (▲) M265IT, (○) M265IV, (□) R26, (■) GA.

(*9*, *22*). The affinities for naphthoquinone (NQ) and three monomethyl-substituted naphthoquinones are summarized in Figure 2 for R26 and GA RCs and for the three M265 mutant RCs. The differences in binding affinities for NQ and methyl-NQ between the two wild-type strains were small—within a factor of 3—but the trends were distinctive. 2- or 6-methyl substitution significantly enhanced binding in both cases, whereas 5-methyl substitution was almost neutral in R26 and actually destabilizing in GA (Figure 2). Identical trends were evident in comparison of 2- and 5-methoxynaphthoquinones (not shown). This distinction between β (2- or 6-methyl NQ) and α (5-methyl NQ) substitution is indicative of the shape constraints of the binding site, as described previously (*9*, *22*). On this basis, the Q_A site of GA appears to be slightly smaller—or more rigid—than that of R26.

All M265 mutant RCs manifested weaker binding than wild-type RCs but still exhibited the distinction between 2- and 5-methyl substitution. The order of effect among the mutant strains was M265IV < M265IT < M265IS. This is consistent with a decrease in van der Waals contact due to the smaller size of the mutant residues at position M265—valine, threonine, and serine vs isoleucine. The smaller effect of the valine substitution as compared to the isosteric threonine may imply that, while the generally lower quinone affinities of the M265 mutant RCs are associated with a greater volume of the binding site, side chain polarity contributes an additional factor. This is also evident in the kinetic behavior.

Rate of $P^+Q_A^-$ Charge Recombination in Wild-Type and M265 Mutant RCs. With native Q-10 as Q_A, the observed

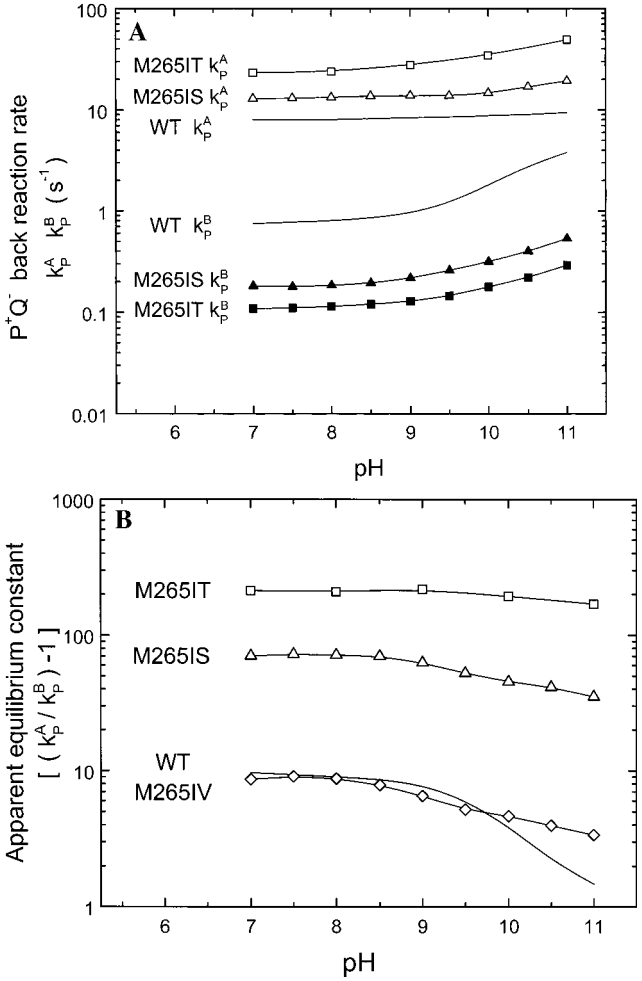

FIGURE 3: pH dependence of the charge recombination reactions. (A) $P^+Q_A^-$ recombination, k_P^A (s^{-1}) (open symbols), and $P^+Q_AQ_B^-$ charge recombination, k_P^B (s^{-1}) (closed symbols), in M265IT (□, ■) and M265IS (△, ▲) mutant RCs, monitored at 430 nm. Wild-type data are shown by the continuous lines (k_P^A, top; k_P^B, bottom). Data for M265IV (not shown) overlapped those for wild type. (B) The *apparent* $P^+Q_A^-Q_B \leftrightarrow P^+Q_AQ_B^-$ electron-transfer equilibrium, $(k_P^A/k_P^B) - 1$, calculated from the data of panel A. M265IT (□), M265IS (△), and M265IV (◇) mutant RCs; continuous line, wild-type RCs. Conditions: 1−2 μM RCs in 2.5 mM KCl, 1 mM buffer (see Methods), 0.02% Triton X-100, 40 μM ubiquinone (Q-10) where present (for k_P^B).

rates of $P^+Q_A^-$ decay (k_P^A) for the two wild-type strains and for M265IV mutant RCs were very similar, while the polar M265 mutant RCs (M265IT and M265IS) were 2−3 times faster (Table 1). With anthraquinone (AQ) and 1-chloro-anthraquinone (1-Cl-AQ), the rates were significantly faster for all RCs. This has been shown previously to be due to the lower redox potentials of these quinones, which allows charge recombination by a thermally activated route via the P^+I^- state (*21*, *28*). With AQ or 1-Cl-AQ as Q_A, the M265IT and M265IS mutant RCs exhibited rates that were 30−100 times faster than wild type, indicating a much lower redox potential in these RCs. In contrast, the M265IV mutant RCs were not significantly different from wild type.

pH Dependence of $P^+Q_A^-$ and $P^+Q_B^-$ Charge Recombination. The rate of decay of P^+ as a function of pH, with and without functional secondary quinone (Q_B), is shown in Figure 3A for the M265 mutant RCs. With Q-10 in both quinone sites, the observed rate of decay of the charge-separated state $P^+Q_B^-$ (k_P^B) was 4−6-fold slower in M265IT

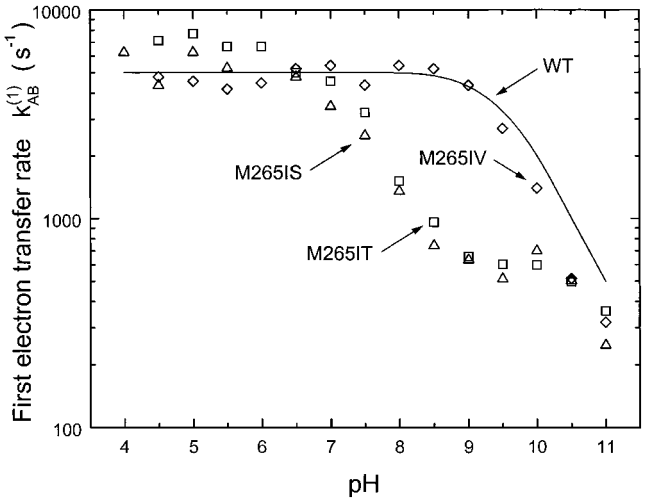

FIGURE 4: pH dependence of the rate of the first electron transfer, $k_{AB}^{(1)}$, in wild-type (continuous line) and mutant RCs: M265IT (□), M265IS (△), and M265IV (◇), measured at 397 nm. Conditions as for Figure 2.

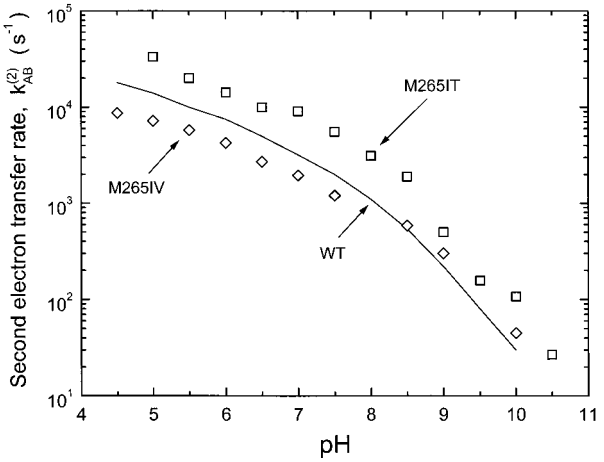

FIGURE 5: pH dependence of the second electron transfer. The rate, $k_{AB}^{(2)}$, in wild-type (continuous line) and M265 mutant RCs, was measured at 450 nm: (□) M265IT mutant RCs; (◇) M265IV mutant RCs. Conditions: 1−2 μM RCs in 2.5 mM KCl, 1 mM buffer (see Methods), 0.02% Triton X-100, 40 μM ubiquinone (Q-10), 2−200 μM ferrocene, depending on pH, plus 0.5 mM potassium ferrocyanide.

and M265IS than in M265IV or wild-type RCs (0.12, 0.19, 1.0, and 0.75 s^{-1}, respectively, at pH 7.0). In contrast, $P^+Q_A^-$ charge recombination (k_P^A) was 2−3 times faster in M265IT and M265IS mutant RCs throughout the pH range. In all respects, M265IV mutant RCs were very similar to wild type. Under appropriate conditions, the relative values of the charge recombination rates of $P^+Q_A^-$ and $P^+Q_B^-$ are a simple indicator of the first electron-transfer equilibrium constant: $L_{AB}^{(1)} \approx k_P^A/k_P^B - 1$ (see ref *1*). Thus, the much larger ratio k_P^A/k_P^B in the polar M265 mutants indicates a substantial increase in the first electron-transfer equilibrium constant, $L_{AB}^{(1)}$ (Figure 3B).

All rates of recombination increased gradually with increasing pH, especially above pH 9. However, the $P^+Q_B^-$ charge recombination in the polar M265 mutant RCs increased less than in the wild-type or M265IV mutant RCs, while the $P^+Q_A^-$ charge recombination accelerated more. Thus, the ratio k_P^A/k_P^B decreased in wild-type and M265IV mutant RCs but was almost pH independent in the polar M265 mutant RCs.

Kinetics of the First Electron Transfer: $Q_A^-Q_B \rightarrow Q_AQ_B^-$. The first electron transfer was qualitatively altered in M265IT and M265IS mutant RCs (Figure 4). In wild-type and M265IV mutant RCs, the kinetics showed a transition from pH independent at pH < 9 to pH dependent at pH > 9. In M265IT mutant RCs, the rate was constant at pH < 7 and similar to the wild-type value ((5−7) × 10^3 s^{-1}), but the onset of pH dependence occurred at much lower pH (≈pH 6.5). A second region of pH independence appeared in the polar mutant RCs at about pH 9, and further pH dependence set in again at about pH 10.5.

Kinetics of the Second Electron Transfer: $Q_A^-Q_B^- \rightarrow Q_AQ_BH_2$. Measurement of the second electron-transfer kinetics at 450 nm, with ferrocene plus ferrocyanide[1] as donor to P^+, showed the rate to be about 4 times faster in the polar M265 mutants than in wild-type or M265IV, at all pH values from 5 to 11 (Figure 5).

In all mutant RCs, oscillations in the Q_B^- semiquinone formation were at least as strong as in wild-type RCs and were notably stronger in the polar M265 mutants, consistent with a large value of $L_{AB}^{(1)}$ and effective transfer of the second electron. In particular, the oscillations remained strong at pH 10, where the wild-type oscillations are almost absent due to the pH-dependent decrease in $L_{AB}^{(1)}$ (*24*, *26*). The magnitude of the oscillations was not significantly affected by the presence or absence of ferrocyanide (not shown).

DISCUSSION

Q_A Binding Site Geometry in M265 Mutant RCs. The behavior of the M265 Q_A site mutants shows that quite subtle changes in the binding site composition can have substantial effects on the physical properties of the site and of the quinone occupant. The binding affinities for various naphthoquinones were significantly weaker in the M265 mutant RCs than in either wild-type strain (GA and R26). This is consistent with the predominantly van der Waals nature of the binding affinity suggested by earlier analyses (*8*, *9*, *22*). Thus, replacement of the native isoleucine by smaller mutant residues makes the Q_A site "looser" (larger or less rigid).

Since M265 points toward one face of the quinone, the steric effect of the mutations is not expected to alter the qualitative response of the site to "edge" substitutions on the quinone ring. Thus, the mutant RCs exhibit the same pattern of binding behavior as do wild-type RCs. In particular, the differences between 2- or 6- (β) and 5- (α) substituted naphthoquinones are consistent with earlier conclusions that the Q_A site is more tightly constrained in the α domain: 5- or 8-monosubstitutions invariably show less affinity gain than other isomers, and 5,8-disubstitution causes catastrophic loss of affinity (*9*).

A small distinction may be evident between M265IT and M265IV mutant RCs, with a slightly greater affinity loss in

[1] In the absence of ferrocyanide, the second electron-transfer kinetics were biphasic (*29*). The amplitudes of the two phases were strongly pH dependent, with the slow phase becoming dominant at high pH with an apparent pK = 6.5 ± 0.1. The rate of the slow phase was only very weakly pH dependent from pH 6 to pH 10.5. This behavior is similar to that seen upon binding certain divalent cations to RCs (*30*). The disappearance of the slow phase in the presence of ferrocyanide suggests that it may be due to ferricenium, produced on the first flash, binding to the RC prior to the second flash.

the former. This would be consistent with the response to the polar mutations including a noncontact effect, such as electrostatic repulsion between the partial charges of the hydroxyl and carbonyl oxygens.

The two wild-type strains, R26 and GA, exhibited slightly different responses to α- and *β*-substituted quinones, with the effect of α-substitution distinctly negative in GA RCs as compared to neutral in R26. This suggests that the R26 Q_A binding site is somewhat larger, or less rigid, than that of GA. Possibly the absence of a bound carotenoid in the RC structure allows the R26 protein to be more flexible globally, including accommodating non-native quinones in the Q_A site.

$P^+Q_A^-$ Recombination Kinetics and the in Situ Midpoint Potential of Q_A. With Q-10 as Q_A, the effect of polar substitution at M265 on the $P^+Q_A^-$ charge recombination rate is a modest 2.5-fold increase, but with AQ or 1-Cl-AQ as Q_A the effect is dramatic. It is well established that the main route for $P^+Q_A^-$ recombination in *Rb. sphaeroides* is by a direct (tunneling) electron transfer from Q_A^- to P^+. However, when a sufficiently low redox potential quinone is active as Q_A a new path is opened in which the electron is thermally excited to the intermediate bacteriopheophytin (I), with subsequent rapid decay from P^+I^- (*21*, *28*):

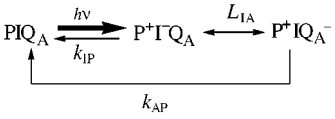

The overall (observed) rate of $P^+Q_A^-$ recombination (P^+ decay) then becomes (see ref *1*)

$$k_P^A = k_{IP}\exp[\Delta G_{IA}/RT] + k_{AP} = k_{IP}/(1 + L_{IA}) + k_{AP}L_{IA}/(1 + L_{IA}) \quad (1)$$

where $\Delta G_{IA} = -RT \ln L_{IA}$ is the free energy gap between I^-Q_A and IQ_A^- and is (largely) determined by the difference in equilibrium redox potentials of I^-/I and Q_A^-/Q_A. Comparison of the rates of $P^+Q_A^-$ recombination, observed with different quinones as Q_A, reveals the value of ΔG_{IA} and allows determination of their relative redox midpoint potentials, assuming that of I^-/I is unchanged (*21*, *28*). k_{IP} is the effective rate of recombination of P^+I^- to the ground state. As discussed by Woodbury et al. (*28*) and Shopes and Wraight (*31*), it is taken here to be 2×10^7 s^{-1}, independent of the chemical identity of Q_A and of the nature of the M265 mutations in the Q_A binding site.

Comparison of Anthraquinone and Ubiquinone Potentials in the Q_A Site. For wild-type RCs with Q-10 as Q_A, $\Delta G_{IA} \approx -470$ meV (*28*), so the first term in eq 1 is only ≈0.3 s^{-1}. Thus, the observed decay of $P^+Q_A^-$, $k_P^A(UQ) = 9.5$ s^{-1}, is essentially equal to k_{AP}, the rate of direct tunneling from Q_A^- to P^+. For wild-type RCs with AQ as Q_A, $k_P^A(AQ) = 129$ s^{-1}. Using the same value for k_{IP} and taking $k_{AP} = 8$ s^{-1} for anthraquinone (*31*, *32*), we obtain $\Delta G_{IA} \approx -305$ meV, implying a value for E_m(AQ) 165 mV more negative than E_m(UQ) in the Q_A site. This is in complete agreement with the difference previously calculated for these two quinones in R26 RCs (*21*, *28*).

For M265IT mutant RCs, the ratio of k_P^A(AQ) to k_P^A(UQ) (6810/25 ≈ 270) gives a first indication that the in situ E_m difference between UQ and AQ is at least 140 mV. However, if we assume, reasonably, that the larger value of k_P^A(UQ) in the mutant as compared to that in the wild type is due to a greater contribution from the activated route (i.e., that k_{AP} is unchanged), then we should compare k_P^A(AQ) in the mutant with k_P^A(UQ) in wild type where the activated route is negligible. In this case, the ratio of rates is 715, corresponding to an E_m difference between UQ and AQ of 165 mV, identical to that estimated above for the wild type. This agreement strongly supports the use of the wild-type value of k_P^A(UQ) and the expectation that the M265 mutations do not significantly alter the structural relationships between Q_A^- and P^+ (electronic factors) that determine the tunneling rate.

Comparison of Mutant and Wild-Type Q_A Potentials. With the same assumption (that the larger value of k_P^A(UQ) in the mutant is due to a greater contribution from the activated route), we can calculate the difference in ΔG_{IA} between the mutant and wild-type RCs (δG_{IA}), with Q-10 as Q_A. Taking the difference in the $P^+Q_A^-$ decay rates ($\Delta k_P = k_P^A$(mut) − k_P^A(wt)), we obtain

$$(\Delta k_P/k_{IP})\exp[-\Delta G_{IA}/RT] + 1 = \exp[\delta G_{IA}/RT] \quad (2)$$

For M265IT mutant RCs with $k_P^A(UQ) = 25$ s^{-1} and wild type (GA) with $k_P^A(UQ) = 9.5$ s^{-1}, this yields a value of $\delta G_{IA} = 110 \pm 5$ meV (using $\Delta G_{IA} = -470$ meV, for UQ as Q_A in the wild type). If all the change resides in Q_A, rather than the bacteriopheophytin, I, this implies that E_m(UQ) in the Q_A site is 110 ± 5 mV lower than in wild-type RCs. For M265IS RCs, the difference is only slightly smaller (with $k_P^A(UQ) = 22$ s^{-1}), and very similar values are obtained from comparisons of the kinetics with 1-Cl-AQ as Q_A.

A similar and more robust estimate can be made from the rates of charge recombination with AQ as Q_A, for which $\Delta G_{IA} = -305$ meV. We find that E_m(AQ) in the Q_A site is 105 mV more negative in M265IT and 80 mV more negative in M265IS than in wild-type RCs. Very similar shifts can be calculated from the empirical relationship derived by Gunner and co-workers on the basis of many artificial quinones as Q_A (*33*) $\Delta E_m = -56.6 \log(k_P^A - 7) - 53.1$ mV.

These are surprisingly large changes in the E_m of Q_A considering the relatively subtle mutational alterations. Hanson and co-workers (*34*), for example, have substituted acidic residues at one or both alanines at M247 and M248 in *Rb. capsulatus* (equivalent to M248 and M249 in *Rb. sphaeroides*), in close proximity to Q_A, with no acceleration in the $P^+Q_A^-$ recombination rate. Although no quinone substitution studies were described, a substantial change in E_m(UQ) might be expected to be detectable in the $P^+Q_A^-$ recombination rate and would certainly be apparent in the rate of decay of $P^+Q_B^-$ (see below).

The lowered Q_A midpoint potentials and weaker quinone binding in the M265 mutant RCs indicate that the semiquinone state is more destabilized in the Q_A site than is the oxidized quinone form. This might arise from a change in the polarity or dielectric of the environment and is consistent with an electrostatic effect of the residue hydroxyl oxygen on the quinone carbonyl oxygen, which would be more marked for the net negatively charged semiquinone. It is not consistent with any significant contribution from a steric

effect on the conformation of the methoxy groups since very similar midpoint potential shifts are seen for both native ubiquinone and anthraquinone.

Decay of $P^+Q_B^-$ and the Free Energy Gap between Q_A/Q_A^- and Q_B/Q_B^-. A very similar kind of analysis applies in the comparison of mutant and wild-type RC behavior for electron transfer to Q_B, and we arrive at similar conclusions. P^+ decay after electron transfer to Q_B can occur via a direct tunneling from Q_B^- to P^+ or by thermal repopulation of $P^+Q_A^-$ followed by recombination (*24*, *26*), as described above:

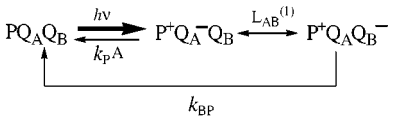

The observed rate of recombination (P^+ decay) is given by (*1*)

$$k_P^B = k_{IP}\exp[\Delta G_{IB}/RT] + k_P^A\exp[\Delta G_{AB}^{(1)}/RT] + k_{BP}$$
$$\approx k_P^A\exp[\Delta G_{AB}^{(1)}/RT] + k_{BP}$$
$$= k_P^A/(1 + L_{AB}^{(1)}) + k_{BP}L_{AB}/(1 + L_{AB}^{(1)}) \quad (3)$$

The term in k_{IP} is negligible ($<0.02\ s^{-1}$) due to the large magnitude of $\Delta G_{IB} \leq -540$ meV. The rate constant for the direct route (k_{BP}) is also small; it has been estimated to be $0.1-0.12\ s^{-1}$ in wild-type RCs at pH 7 (*27*) and $0.04-0.06\ s^{-1}$ in L213DN mutant RCs where aspartic acid at position L213 is replaced by asparagine (*19*, *35*). This is 100 times smaller than k_P^A, and the term in k_{BP} can be largely ignored so long as $L_{AB}^{(1)}$ is not too large. This is adequate for wild-type RCs where $L_{AB}^{(1)} \approx 15$. Thus, the observed decay of $P^+Q_B^-$ in wild-type RCs is about 10 times faster than k_{BP} and k_P^B can be used as a simple and direct assay of $L_{AB}^{(1)}$, according to

$$L_{AB}^{(1)} \approx k_P^A/k_P^B - 1$$

However, in the polar M265 mutants the observed P^+ decay is much slower and is comparable to the expected value of k_{BP}. Thus, the ratio of the rates of decay of $P^+Q_A^-$ and $P^+Q_B^-$ yields only a lower limit to the free energy difference between Q_A^-/Q_A and Q_B^-/Q_B.

For M265IT and M265IS mutant RCs, respectively, the values of $k_P^A/k_P^B - 1$ are at least 25 and 8 times larger than wild type at pH 8, corresponding to increases in the free energy gap between $Q_A^-Q_B$ and $Q_AQ_B^-$ of not less than 80 and 50 mV. These are significantly smaller than the shifts in the E_m of Q_A estimated above due to the inadequacy of ignoring the direct back reaction route for $P^+Q_B^-$. This is also suggested by the fact that the apparent value of $L_{AB}^{(1)}$, i.e., $k_P^A/k_P^B - 1$, is almost pH independent in the polar M265 mutant RCs, in contrast to the wild type where the free energy gap decreases ($\Delta G_{AB}^{(1)}$ becomes less negative) at pH values above 9. Thus, it seems likely that $\Delta G_{AB}^{(1)}$ changes in M265IT by about 100 mV, in accordance with the midpoint potential of Q_A, while the properties of the Q_B pocket are largely unaffected by the M265 mutations in the Q_A site.

First Electron Transfer. The rate of electron transfer from Q_A^- to Q_B in wild-type RCs is characterized by pH independence from pH 4 to pH 9, above which the rate decreases in a manner consistent with a p*K* of about 9.5 (*24*, *26*). This behavior has been ascribed to the ionization state of a cluster of acidic residues close to Q_B, including glutamate L212 (Glu^{L212}), with an unusually high effective p*K* (*19*, *36*). Electron transfer to Q_B is considered to be modulated by the electrostatic potential generated in the Q_B site by the ionization state of these residues (*1*, *37*−*41*). The rate of electron transfer is then determined by the fraction of ionizable species in the protonated (neutral) state, which, above the apparent p*K*, decreases in proportion to the pH.

This picture is broadly supported by structure-based electrostatic calculations at various levels of sophistication (*42*−*46*), which show strong interactions within a substantial, ionizable residue cluster leading to internal buffer-like activity. The ionization equilibria are clearly distributed over several residues, including Glu^{L212}, but these molecular level analyses are still ambiguous in their identification of the titration behavior of individual residues. Nevertheless, all the residues identified as contributing significantly to the energetics of electron transfer from Q_A to Q_B are physically located in the Q_B binding domain and its immediate surroundings. It is therefore surprising to find that mutation of M265 in the Q_A pocket causes a rather dramatic change in the pH dependence of the rate of the first electron transfer.

In the polar M265 mutant RCs, the rate is essentially unaltered at low pH, where the local electrostatics of the Q_B site are optimal, but onset of pH dependence occurs at about pH 6.5, at least 2 units lower than in the wild type (Figure 4). As for the wild type, this may be taken to indicate that rapid electron transfer occurs from a protonated state, the population of which decreases above the p*K*. The reappearance of pH independence at about pH 9 may then reveal the slower intrinsic rate of the deprotonated state (Scheme 1).

Scheme 1

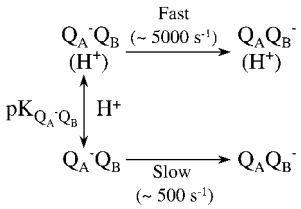

In the formalism of a single ionizable entity responsible for each region of pH dependence, the onset of pH dependence in this mutant corresponds to $pK_{Q_A^-Q_B} = 7.2$, with Q_B oxidized.

In wild-type RCs, the onset of pH dependence corresponds to an apparent $pK_{Q_A^-Q_B} \approx 9.6$. A flattening of the pH dependence is detectable above pH 11, but this is unrevealing as it is expected for the observed rate of equilibration, i.e., the sum of the forward and reverse rate constants, $k_{ET}^{(1)} = k_{AB}^{(1)} + k_{BA}^{(1)}$, which cannot be less than the smaller of $k_{AB}^{(1)}$ and $k_{BA}^{(1)}$. If $k_{BA}^{(1)}$ is pH independent, the plot of log $k_{ET}^{(1)}$ vs pH will deviate from linearity as $k_{AB}^{(1)}$ approaches $k_{BA}^{(1)}$ at high pH. This occurs when the pH dependent equilibrium constant, $L_{AB}^{(1)}$, approaches 1 and, in wild-type RCs, $L_{AB}^{(1)}$ can be independently obtained from the kinetics of the $P^+Q_B^-$ charge recombination. The pH dependence of $L_{AB}^{(1)}$ reveals $pK_{Q_A^-Q_B} \approx 9.9$ and $pK_{Q_AQ_B^-} \approx 11.4$ (*1*, *19*, *26*). (These values are somewhat, but not markedly, dependent on conditions, including ionic strength.) With this, the rate of electron

transfer in the deprotonated state of the wild-type acid cluster at pH > 11.5 is still poorly defined but may be estimated at $\leq 50\ s^{-1}$.

In contrast to wild type, in M265IT and M265IS mutant RCs, $P^+Q_B^-$ recombination proceeds largely by the direct route and does not reflect the equilibrium between $Q_AQ_B^-$ and $Q_A^-Q_B$. Thus, at the present time, we do not have an easy experimental handle on the pH dependence of $L_{AB}^{(1)}$. However, it is clear that the onset of pH independence of the kinetics at pH 8.5 is *not* due to approaching equivalence of $k_{AB}^{(1)}$ and $k_{BA}^{(1)}$ as the equilibrium constant is still large at this pH. Thus, the pH independent rate, between pH 8.5 and pH 10.5, does indeed represent electron transfer in the deprotonated state, as in Scheme 1. The rate is significant ($\approx 500\ s^{-1}$) and quite distinct from the high pH limit in wild-type RCs ($\leq 50\ s^{-1}$). Thus, if the lower onset of pH dependence in the mutant RCs is interpreted as a downshift in the p*K* behavior of the acid cluster, it is not clear why the population of the protonated state loses control of the process at such a high value of the rate constant. This may indicate that two processes are also at work in the wild-type behavior but are merged at the higher pH. Consistent with this, a second region of pH dependence in M265IT mutant RCs sets in at pH 10.5, and the rate appears to merge with wild-type values at pH ≥ 11. The high pH behavior in the mutant, therefore, may not represent a second p*K* but only the intersection with a greater rate limitation common to both mutant and wild type, such as the wild-type p*K* process above pH 9.6.

Transfer of the first electron to Q_B has become much more interesting with the observation that the quinone might not be in the binding pocket in the dark adapted state, but may favor localization in an ante-chamber some 5 Å distal to the functional binding site (*7*). This raises possibilities for gating activities involving translation of the quinone headgroup (*47*), which then becomes tightly bound in the "proximal" position upon reduction to the semiquinone, but the relevance of such proposals has yet to be established. Variability in the X-ray structural data (*6*, *7*, *48*) and in the kinetics of the first electron transfer (*49*−*51*) suggests that their relative occupancies may be easily perturbed. Thus, the affinities of these two positions may be very similar. A computational assessment of the two positions also gave very similar values for the binding energies (*52*).

As discussed below, preliminary FTIR studies indicate very little structural alteration in any of the M265 mutants. Thus, the 10-fold slowing of the first electron transfer process in the polar M265 mutants is unlikely to arise from a direct influence on the electron-transfer rate, per se, for example via the distance or strength of coupling between Q_A and Q_B. In fact, the $Q_A^-Q_B \rightarrow Q_AQ_B^-$ reaction in wild-type RCs has been shown to be not rate limited by electron transfer (*47*).

The rather dramatic effect of the polar M265 Q_A-site mutations on the first electron transfer could instead arise from a relatively minor influence on the equilibrium between distal and proximal states or on the kinetics of interconversion. In particular, the unusual pH dependence of the first electron-transfer kinetics could reflect a shift in the pH dependence of Q_B binding in the proximal position. Because there are few ionizable residues close to Q_A, the primary influences of Q_A/Q_A^- on ionization equilibria of the protein are focused in the Q_B binding domain (*46*).

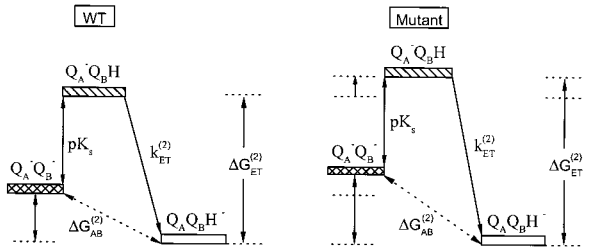

FIGURE 6: Influence of the redox midpoint potential of Q_A on the energetics of the second electron transfer. Lowering $E_m(Q_A)$ raises the free energy of $Q_A^-Q_B^-$ and $Q_A^-Q_BH$ but does not affect that of $Q_AQ_BH^-$. Thus, the p*K* of the semiquinone (pK_s) is unchanged, while the driving force for electron transfer ($\Delta G_{ET}^{(2)}$) is increased.

Second Electron Transfer. Transfer of the second electron to Q_B is tightly coupled to delivery of a proton to the quinone headgroup. This can occur in one of two sequences (top right or bottom left in Scheme 2). In wild-type RCs, Graige et al.

Scheme 2

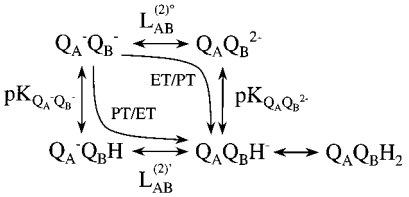

(*53*) have provided strong evidence for the lower route, in which electron transfer follows proton transfer (PT/ET). The electron transfer is rate limiting, but the net rate is modulated by the pH-dependent equilibrium population of the protonated semiquinone of Q_B (Q_BH). This implies rapid protonation equilibration, which was estimated to be greater than $10^7\ s^{-1}$ at pH 7.5 (*53*, *54*). The rate-limiting nature of the electron transfer was indicated by its dependence on the electron driving force, i.e., the redox potential of various quinone analogues in the Q_A site.

In the polar M265 mutant RCs, the rate of the second electron transfer was 3−4 times faster than in the wild type, at all pH values from pH 4 to pH 11 (Figure 5). This is fully consistent with the model of Graige et al. (*53*). The observed acceleration is roughly as expected if the 100 mV lower E_m of Q_A provides an equivalently larger driving force for electron transfer (Figure 6).

Origin of the Shift in E_m of Q_A/Q_A^-. The effect that mutational substitution of Ile^{M265} has on the E_m of Q_A is unexpectedly large ($\Delta E_m = -100$ mV for M265IT) and initially invited speculation on the role of the methoxy group orientation. Several computational studies have shown this to be a significant source of variation in redox and acid−base properties of methoxy quinones (*11*−*15*, *55*). However, the observation that the E_m shift for Q_A in the M265 polar mutants is very similar for native ubiquinone-10 and for anthraquinone as Q_A eliminates this as a possible origin of this mutant effect.

The negligible effect of substituting valine for the native isoleucine indicates that the absence of the δ-methyl group of Ile^{M265}, which is closest to C5 and C6 and their substituents (the C5′-methyl group and the first isoprene unit), has no impact on the midpoint potential of ubiquinone in the Q_A site. Instead, attention is focused on the polar nature of threonine and serine, where a hydroxyl is in the γ-position of the side chain. There are few precedents to draw upon,

although the mutational *removal* of a hydroxyl group can disrupt structurally important hydrogen bonding features. In $P450_{cam}$, replacement of threonine 252 by alanine breaks a bond that is important in holding a backbone twist and allows rearrangement of water molecules near the active site (*56*). In cytochrome *c*, substitution of a phenylalanine for tyrosine 67 releases a conserved water molecule and allows a more stable structure to be obtained (*57*).

In terms of more diverse hydrogen bonding partners, Lin et al. (*58*) mutated RCs from *Rb. sphaeroides* to add or remove histidines at sites around the bacteriochlorophyll dimer. The effect on the primary donor was substantial but, in apparent contrast to our findings on Q_A, adding hydrogen bond donors *increased* the E_m of P/P^+ roughly linearly by about 90 mV per bond.

The equally large *decrease* in the E_m of Q_A^-/Q_A in the polar M265 mutants might arise from several distinct mechanisms. One possibility is the introduction of a water molecule to the Q_A site, stabilized by hydrogen bonding to the threonine or serine hydroxyl. This cannot be easily ruled out, but there are no water moleules in the native Q_A pocket and few opportunities for a new water molecule to make the number of hydrogen bonds usually required to stabilize internal waters. Also, the space created by the mutations is mostly over the C5, C6, and C1 carbons, and an incorporated water molecule might be most likely to influence the C1═O frequency. In contrast, our preliminary FTIR studies show only a small effect on the C4═O mode (T. A. Wells, E. Takahashi, and C. A. Wraight, manuscript in preparation).

Alternatively, the effect of the γ-hydroxyl of threonine or serine on the quinone or semiquinone states might arise either from hydrogen bonding or from the OH partial charges (or dipole). The structural context for this may be derived from the native isoleucine, with two γ-carbons, the positions of which are evident in the available X-ray structures (*6*, *7*). The methylene group is within 4 Å of the C4 carbonyl group of Q_A and N_δ (NH) of histidine M219. The γ-methyl of isoleucine is only within 4 Å of the C3′-methoxy carbon of Q_A and C_ϵ of His^{M219}. Rotation around the $C_\alpha-C_\beta$ bond can only significantly shorten the distance from a γ-substituent to the histidine N_δ.

Although the γ-position to carbonyl oxygen distance might be feasible for hydrogen bonding, without significant structural changes the possible angles are very unsuitable. Furthermore, a normal hydrogen bonding interaction with the carbonyl would be likely to stabilize the semiquinone, raising the E_m rather than lowering it. Similarly, orientation of the positive end of the OH dipole toward the quinone would also stabilize the semiquinone anion. On the other hand, the repulsive electrostatic interaction between a negative partial charge of the hydroxyl oxygen and the semiquinone anion would lower the E_m. A similar but weaker interaction with the partial charge of the carbonyl oxygen could also account for a slightly lower affinity for neutral quinone in the polar mutants as compared to the valine substitution. The difference between M265IT and M265IV RCs is small (0.3−0.4 kcal/mol) and easily within the range of an interaction between the partial charges of OH and C═O oxygens at a distance of about 4 Å.

The possible angles between a γ-hydroxyl at residue M265 and the nitrogen (N_δ) of histidine-M219 are much more suitable for hydrogen bonding, and the effects of the polar mutants might therefore arise from weakening of the hydrogen bond between the histidine and quinone by competition from the hydroxyl oxygen as a hydrogen bond *acceptor* from the histidine $N_\delta H$. This also would be consistent with the slightly weaker quinone affinity of the polar mutants as compared to the valine mutant and could reasonably destabilize the semiquinone more than the quinone, resulting in a lower E_m.

An alternative interaction to consider might be between the γ-hydroxyl and the π electron system of the quinonoid ring. The existence and significance of π-hydrogen bonds is well-known from model compounds, but their energetic consequences are varied and hard to predict (*59*).

Infrared spectroscopy could be expected to yield some insight on the nature of the side chain-quinone interaction, and we have found a small but distinct 3−4 cm^{-1} upshift in the carbonyl stretch associated with the C-4 carbonyl (at 1601 cm^{-1} in wild type) (T. A. Wells, E. Takahashi, and C. A. Wraight, manuscript in preparation). The identification of this band as predominantly a C4═O mode has been strongly supported by isotopic substitutions (*60*−*62*), but the origin of the unusually low frequency for a carbonyl stretch is not understood. Strong hydrogen bonding to histidine-M219 has been proposed but is unlikely to fully account for it. It is also not readily consistent with the lack of response of this vibration to deuterium exchange, whereas the semiquinone IR bands do respond (*63*).

The upshift in the 1601 cm^{-1} band is seen only in the polar mutants and not in M265IV. It is consistent with either an electrochromic effect arising from the hydroxyl partial charges or dipole or a weakening of the hydrogen bond between C4═O and His^{M219}. Electrochromic bandshifts in reaction center IR spectra have been reported by Breton and Nabedryk (*64*) but are not in any sense calibrated. IR frequency shifts due to hydrogen bonding have been extensively studied, with the general result that the carbonyl stretch is only moderately sensitive (*65*). Empirical relationships have been derived and one such calibration for carbonyls yields $E_{hb} = -250\Delta\nu_{C=O}/\nu_{C=O}$ kcal/mol (*66*). On this basis, the upshift in the C4═O carbonyl mode observed here corresponds to a decrease in hydrogen bond strength of about 0.3−0.4 kcal/mol. This is in good, but possibly coincidental, agreement with the difference in binding affinity between the valine and threonine mutant RCs.

ACKNOWLEDGMENT

We thank Dr. Kurt Warncke (now at Emory University, Atlanta, GA) for some early measurements of quinone binding to the M265 mutant RCs.

REFERENCES

1. Shinkarev, V. P., and Wraight, C. A. (1993) in *The Photosynthetic Reaction Center* (Deisenhofer, J., and Norris, J. R., Eds.) pp 193−255, Academic Press, San Diego.
2. Okamura, M. Y., and Feher, G. (1995) in *Advances in Photosynthesis* (Blankenship, R., Madigan, M., and Bauer, C., Eds.) pp 577−593, Kluwer Academic Publishers, Dordrecht, The Netherlands.
3. Wraight, C. A. (1998) in *Photosynthesis: Mechanisms and Effects* (Garab, G., Ed.) pp 693−698, Kluwer Academic Publishers, Dordrecht, The Netherlands.
4. Allen, J. P., Feher, G., Yeates, T. O., Komiya, H., and Rees, D. C. (1988) *Proc. Natl. Acad. Sci. U.S.A. 85*, 8487−8491.

5. El-Kabbani, O., Chang, C.-H., Tiede, D., Norris, J., and Schiffer, M. (1991) *Biochemistry 30*, 5361−5369.
6. Ermler, U., Fritzsch, G., Buchanan, S. K., and Michel, H. (1994) *Curr. Biol. Struct. 2*, 925−936.
7. Stowell, M. H. B., McPhillips, T. M., Rees, D. C., Soltis, S. M., Abresch, E., and Feher, G. (1997) *Science 276*, 812−816.
8. Gunner, M. R., Tiede, D. M., Prince, R. C., and Dutton, P. L. (1982) in *Function of Quinones in Energy Conserving Systems* (Trumpower, B. L., Ed.) pp 265−269, Academic Press, New York.
9. Gunner, M. R., Braun, B. S., Bruce, J. M., and Dutton, P. L. (1985) in *Antennas and Reaction Centers of Photosynthetic Bacteria: Structure, Interactions and Dynamics* (Michel-Beyerle, M. E., Ed.) pp 298−304, Springer-Verlag, Berlin.
10. Warncke, K., and Dutton, P. L. (1993) *Proc. Natl. Acad. Sci. U.S.A. 90*, 2920−2924.
11. Prince, R. C., Dutton, P. L., and Bruce, J. M. (1983) *FEBS Lett. 160*, 273−276.
12. Prince, R. C., Halbert, T. R., and Upton, T. H. (1988) in *Advances in Membrane Biochemistry and Bioenergetics* (Kim, C. H., Tedeschi, H., Diwan, J. J., and Salerno, J. C., Eds.) pp 469−478, Plenum Press, New York.
13. Robinson, H. H., and Kahn, S. D. (1990) *J. Am. Chem. Soc. 112*, 4728−4731.
14. Nonella, M. (1998) *Photosynth. Res. 55*, 253−259.
15. Nonella, M., and Brändli, C. (1996) *J. Phys. Chem. 100*, 14549−14559.
16. McComb, J. C., Stein, R. R., and Wraight, C. A. (1990) *Biochim. Biophys. Acta 1015*, 156−171.
17. Takahashi, E., Maróti, P., and Wraight, C. A. (1990) in *Current Research in Photosynthesis* (Baltscheffsky, M., Ed.) pp 169−172, Kluwer Academic Publishers, Dordrecht, The Netherlands.
18. Kunkel, T. A. (1985) *Proc. Natl. Acad. Sci. U.S.A. 82*, 488−492.
19. Takahashi, E., and Wraight, C. A. (1992) *Biochemistry 31*, 855−866.
20. Okamura, M. Y., Isaacson, R. A., and Feher, G. (1975) *Proc. Natl. Acad. Sci. U.S.A. 72*, 3492−3496.
21. Gunner, M. R., Robertson, D. E., and Dutton, P. L. (1986) *J. Phys. Chem. 90*, 3783−3795.
22. Warncke, K., and Dutton, P. L. (1993) *Biochemistry 32*, 4769−4779.
23. Warncke, K., Gunner, M. R., Braun, B. S., Gu, L., Yu, C.-A., Bruce, J. M., and Dutton, P. L. (1994) *Biochemistry 33*, 7830−7841.
24. Wraight, C. A. (1979) *Biochim. Biophys. Acta 548*, 309−327.
25. Wraight, C. A., and Stein, R. R. (1980) *FEBS Lett. 113*, 73−77.
26. Kleinfeld, D., Okamura, M. Y., and Feher, G. (1984) *Biochim. Biophys. Acta 766*, 126−140.
27. Labahn, A., Bruce, J. M., Okamura, M. Y., and Feher, G. (1995) *Chem. Phys. 97*, 355−366.
28. Woodbury, N. W., Parson, W. W., Gunner, M. R., Prince, R. C., and Dutton, P. L. (1986) *Biochim. Biophys. Acta 851*, 6−22.
29. Takahashi, E., Wells, T. A., and Wraight, C. A. (1998) in *Photosynthesis: Mechanisms and Effects* (Garab, G. Z., Ed.) pp 853−856, Kluwer Academic Publishers, Dordrecht, The Netherlands.
30. Paddock, M. L., Graige, M. S., Feher, G., and Okamura, M. Y. (1999) *Proc. Natl. Acad. Sci. U.S.A. 96*, 6183−6188.
31. Shopes, R. J., and Wraight, C. A. (1987) *Biochim. Biophys. Acta 893*, 409−425.
32. Sebban, P., and Wraight, C. A. (1989) *Biochim. Biophys. Acta 974*, 54−65.
33. Gunner, M. R., and Dutton, P. L. (1989) *J. Am. Chem. Soc. 111*, 3400−3412.
34. Valerio-Lepiniec, M., Miksovska, J., Schiffer, M., Hanson, D. K., and Sebban, P. (1999) *Biochemistry 38*, 390−398.
35. Labahn, A., Paddock, M. L., McPherson, P. H., Okamura, M. Y., and Feher, G. (1994) *J. Phys. Chem. 98*, 3417−3423.
36. Paddock, M. L., Rongey, S. H., Feher, G., and Okamura, M. Y. (1989) *Proc. Natl. Acad. Sci. U.S.A. 86*, 6602−6606.
37. Hanson, D. K., Tiede, D. M., Nance, S. L., Chang, C.-H., and Schiffer, M. (1993) *Proc. Natl. Acad. Sci. U.S.A. 90*, 8929−8933.
38. Rongey, S. H., Paddock, M. L., Feher, G., and Okamura, M. Y. (1993) *Proc. Natl. Acad. Sci. U.S.A. 90*, 1325−1329.
39. Maróti, P., Hanson, D. K., Baciou, L., Marianne, S., and Sebban, P. (1994) *Proc. Natl. Acad. Sci. U.S.A. 91*, 5617−5621.
40. Sebban, P., Maróti, P., Schiffer, M., and Hanson, D. K. (1995) *Biochemistry 34*, 8390−8397.
41. Takahashi, E., and Wraight, C. A. (1996) *Proc. Natl. Acad. Sci. U.S.A. 93*, 2640−2645.
42. Beroza, P., Fredkin, D. R., Okamura, M. Y., and Feher, G. (1991) *Proc. Natl. Acad. Sci. U.S.A. 88*, 5804−5808.
43. Beroza, P., Fredkin, D. R., Okamura, M. Y., and Feher, R. (1995) *Biophys. J. 68*, 2233−2250.
44. Gunner, M. R., and Honig, B. (1992) in *The Photosynthetic Bacterial Reaction Center: Structure, Spectroscopy and Dynamics II* (Breton, J., and Verméglio, A., Eds.) pp 403−410, Plenum, New York.
45. Lancaster, C. R. D., Michel, H., Honig, B., and Gunner, M. R. (1996) *Biophys. J. 70*, 2469−2492.
46. Alexov, E. G., and Gunner, M. R. (1997) *Biophys. J. 74*, 2075−2093.
47. Graige, M. S., Feher, G., and Okamura, M. Y. (1998) *Proc. Natl. Acad. Sci. U.S.A. 95*, 11679−11684.
48. Lancaster, C. R. D., and Michel, H. (1996) *Photosynth. Res. 48*, 65−74.
49. Takahashi, E., Maróti, P., and Wraight, C. A. (1992) in *Electron and Proton Transfer in Chemistry and Biology* (Diemann, E., Junge, W., Müller, A., and Ratazczak, H., Eds.) pp 219−236, Elsevier, Amsterdam.
50. Tiede, D. M., Vazquez, J., Cordova, J., and Marone, P. A. (1996) *Biochemistry 35*, 10763−10775.
51. Utschig, L. M., Ohigashi, Y., Thurnauer, M. C., and Tiede, D. M. (1998) *Biochemistry 37*, 8278−8281.
52. Grafton, A. K., and Wheeler, R. A. (1999) *J. Phys. Chem. B 103*, 5380−5387.
53. Graige, M. S., Paddock, M. L., Bruce, J. M., Feher, G., and Okamura, M. Y. (1996) *J. Am. Chem. Soc. 118*, 9005−9016.
54. Paddock, M. L., Senft, M. E., Graige, M. S., Rongey, S. H., Turanchik, T., Feher, G., and Okamura, M. Y. (1998) *Photosynth. Res. 55*, 281−291.
55. Burie, J.-R., Boullais, C., Nonella, M., Mioskowski, C., Nabedryk, E., and Breton, J. (1997) *J. Phys. Chem. B 101*, 6607−6617.
56. Raag, R., Martinis, S. A., Sligar, S. G., and Poulos, T. L. (1991) *Biochemistry 30*, 11420−11429.
57. Luntz, T. L., Schejter, A., Garber, E. A. E., and Margoliash, E. (1989) *Proc. Natl. Acad. Sci. U.S.A. 86*, 3524−3528.
58. Lin, X., Murchison, H. A., Nagarajan, V., Parson, W. W., Allen, J. P., and Williams, J. C. (1994) *Proc. Natl. Acad. Sci. U.S.A. 91*, 10265−10269.
59. Engdahl, A., and Nelander, B. (1985) *Chem. Phys. Lett. 113*, 49−55.
60. Breton, J., Burie, J.-R., Berthomieu, C., Berger, G., and Nabedryk, E. (1994) *Biochemistry 33*, 4953−4965.
61. Breton, J., and Nabedryk, E. (1996) *Biochim. Biophys. Acta 1275*, 84−90.
62. Brudler, R., de Groot, J. M., van Liemt, W. B. S., Steggerda, W. F., Esmeijer, R., Gast, P., Hoff, A. J., Lugtenburg, J., and Gerwert, K. (1994) *EMBO J. 13*, 5523−5530.
63. Breton, J., and Nabedryk, E. (1995) in *Photosynthesis: From Light to Biosphere* (Mathis, P., Ed.) pp 395−400, Kluwer Academic Publishers, Dordrecht, The Netherlands.
64. Breton, J., Nabedryk, E., Allen, J. P., and Williams, J. C. (1997) *Biochemistry 36*, 4515−4525.
65. Bellamy, L. J. (1968) *Advances in Infrared Group Frequencies*, Methuen & Co., Ltd., London.
66. Zadorozhnyi, B. A., and Ishchenko, I. K. (1965) *Opt. Spectrosc. (Engl. Trans.) 19*, 306−308.

BI001055G